NEUROSCIENCE

Suppressing feedback signals to visual cortex abolishes attentional modulation

Samantha R. Debes[1] and Valentin Dragoi[1,2]*

Attention improves perception by enhancing the neural encoding of sensory information. A long-standing hypothesis is that cortical feedback projections carry top-down signals to influence sensory coding. However, this hypothesis has never been tested to establish causal links. We used viral tools to label feedback connections from cortical area V4 targeting early visual cortex (area V1). While monkeys performed a visual–spatial attention task, inactivating feedback axonal terminals in V1 without altering local intracortical and feedforward inputs reduced the response gain of single cells and impaired the accuracy of neural populations for encoding external stimuli. These effects are primarily manifested in the superficial layers of V1 and propagate to downstream area V4. Attention enhances sensory coding across visual cortex by specifically altering the strength of corticocortical feedback in a layer-dependent manner.

Selective attention is a critical brain mechanism that enhances the processing of relevant sensory information. Attentional modulation of sensory encoding, intensively studied over the past several decades, has long been hypothesized to originate from downstream areas carrying top-down feedback signals to early cortex such as to increase response gain, sensitivity, and accuracy of network computations (*1*–*4*). Understanding the neural mechanisms of attentional modulation depends on our ability to activate or silence presynaptic downstream areas and subsequently assess their impact on the target network. However, separating the impact of feedback inputs from local intracortical and bottom-up inputs, which is necessary for examining the mechanism of top-down attentional modulation, has been challenging when using traditional neuromodulation methods (*1*–*11*). Here, we combined in vivo electrophysiology in behaving monkeys with an optogenetic protocol to perturb construct-expressing neuronal processes and modulate feedback signals without altering the strength of feedforward and intracortical inputs that are not directly caused by feedback.

To examine the function of corticocortical feedback for attentional modulation of sensory coding, we have chosen a major pathway involving primary and midlevel visual cortical areas V1 and V4 in behaving monkeys. Neurons in V4 carry top-down signals related to behavioral context and attention to V1 via direct, monosynaptic feedback projections (*12*–*16*). Although V1 also receives feedback inputs from area V2, neurons in V4 are more strongly modulated by attention and are hierarchically closer to decision-making areas; hence, they are ideally suited to examine the impact of cortical feedback on the transmission of attentional signals to early cortex (*17*, *18*).

[1]Department of Neurobiology and Anatomy, McGovern Medical School, University of Texas at Houston, Houston, TX 77030, USA. [2]Department of Electrical and Computer Engineering, Rice University, Houston, TX 77005, USA.
*Corresponding author: Email: valentin.dragoi@uth.tmc.edu

Results

We developed a sensitive assay based on viral-mediated labeling of feedback connections arising from midlevel cortical area V4 that target area V1. The construct leveraged a halorhodopsin-derived chloride pump, Jaws, in adeno-associated virus serotype 8 (AAV8) under the control of the promoter human synapsin (*19*, *20*). AAV8-hSyn-Jaws-GFP-ER2 was expressed within an approximately 12.6-mm^3 cortical volume in area V4 (Fig. 1A) (see materials and methods). This allowed us to simultaneously place a linear electrode array and fiber optic in V1 to record neural activity at multiple sites (fig. S1) and selectively suppress axonal feedback terminals of V4 neurons targeting V1 while macaques performed a spatial attention task. Because the viral construct was injected in V4, we reasoned that shining red light in the superficial layers of V1 would specifically inactivate feedback inputs while leaving unperturbed local intracortical and feedforward inputs to V1 neurons (Fig. 1A). This allowed us to examine whether the attentional modulation of neural populations in V1 is impaired when suppressing cortical feedback from V4 and whether the hypothesized reduction in attentional modulation in V1 is further transmitted to postsynaptic V4 targets.

Optogenetic suppression of V4 feedback axons in V1

Two monkeys performed a spatial-attention contrast detection task (Fig. 1B and fig. S2) whereby various contrast stimuli were displayed at two symmetric spatial locations on a computer screen. One location covered the receptive fields of the neurons being recorded and the other location was outside the receptive fields, diametrically opposed at the same eccentricity. Only one spatial location was behaviorally relevant on a given trial: Monkeys were cued by the color of the fixation point to attend to the stimuli covering the neurons' receptive fields or to those presented on the contralateral side (see materials and methods) (Fig. 1B). On 50% of trials in each condition, optical stimulation was applied to selectively suppress V4 feedback axons in the upper layers of V1. To maintain equal behavioral performance in the "laser" and control conditions, we restricted laser power to a low level such that behavioral performance at the attended side was not significantly different between control and laser trials (P = 0.52) (Fig. 1B); these effects were consistent across animals (fig. S3), and perceptual performance was unaffected by the stimuli flashed at the unattended location (fig. S4). If light stimulation would change behavioral performance across conditions, the obtained unequal reward across conditions could possibly alter behavioral context and hence introduce additional top-down feedback signals besides those related to attention. The lack of a behavioral effect in the laser condition may be due to the fact that in monkey cortex, only a fraction of neurons at the injection site are typically transfected (*21*), and this likely resulted in a small number of cells that were perturbed relative to the entire V1 population encoding the stimuli.

We first placed the electrode array and fiber optic at the injection site in V4, which was associated with a direct suppression of local neural activity ($P = 4.22 \times 10^{-5}$) (Fig. 1C and fig. S6). When the recording array and fiber optic were placed at the V1 sites with overlapping receptive fields corresponding to the V4 injection sites, responses were significantly reduced, indicating a selective suppression of V4 axons terminating in V1 ($P = 3.85 \times 10^{-10}$) (Fig. 1D and fig. S5). We confirmed that the differences in firing rates seen in V1 indeed reflect feedback modulation and hence performed electrical recordings in a control, likely nontransfected area (P = 0.44) (Fig. 1E). When we separated the electrode and fiber optic by several millimeters, V1 responses were not influenced by light (P = 0.84) (Fig. 1F). Light stimulation presented either alone or in combination with the visual stimulus did not change the mean eye position, eye velocity, or pupil size across trials (median eye X position, P = 0.75; median eye Y position, P = 0.71; median pupil size, P = 0.69; median eye X velocity, P = 0.68; median eye Y velocity, P = 0.73, Wilcoxon rank sum test) (fig. S7).

V4 feedback pathways carry attentional signals to V1

We examined the role of cortical feedback in modulating attentional effects in V1 and isolated 239 neurons recorded across 16 sessions in two animals (Fig. 2A) that were both stimulus and light sensitive ($P < 0.05$, Wilcoxon rank sum test). If feedback projections carry attentional signals, inactivating axonal terminals

in V1 would significantly reduce the strength of attentional modulation such that the responses of V1 cells in the attended laser condition would be indistinguishable from those in the unattended laser condition. Without laser stimulation (control, Fig. 2A, left), there was a 7.2% (±2.06) increase in neurons' mean firing rates when high-contrast stimuli were attended (relative to unattended, $P = 9.59 \times 10^{-10}$) (*22*–*25*). However, when we inactivated axonal feedback terminals (Fig. 2A, middle), the responses of neurons in the attended and unattended conditions became indistinguishable ($P = 0.95$). Attentional modulation was abolished when cortical feedback was inactivated [high-contrast, $P = 3.61 \times 10^{-9}$ (Fig. 2A, right, and fig. S8), i.e., a 7.4-fold decrease in attentional modulation]; the interaction between laser stimulation and attention was statistically significant ($P = 0.0022$, Kruskal-Wallis test, post hoc Fisher's least significant difference test). This result was also significant when computed by electrode penetration (fig. S9). In the absence of attention, there was no significant difference between laser and control firing rates ($P = 0.057$, Wilcoxon signed-rank test).

Despite expectation that attention is most needed when stimuli are difficult to see, neuronal responses were primarily modulated at the highest stimulus contrast (Fig. 2, B and C, and fig. S10). When cortical feedback inputs from V4 were inactivated, we found a lack of attentional modulation across all contrasts ($P = 0.18$, Wilcoxon signed-rank test). However, although firing rates were only weakly modulated by attention at low stimulus contrasts, a linear decoder (classifying stimulus-present versus stimulus-absent trials) based on the population response in each session yielded a significant improvement in decoder accuracy when feedback signals were present [attended versus unattended conditions: low-contrast (c1-c2), $P = 0.0061$; high-contrast (c3-c4), $P = 0.00053$ (Fig. 2D)]. Inactivating cortical feedback inputs rendered decoder performance indistinguishable between attended and unattended conditions (low-contrast, $P = 0.38$; high-contrast, $P = 0.50$). The relative difference in decoder performance (attended versus unattended) was significantly larger in control compared to laser condition (relative difference: low-contrast, decreased by 87.8%, $P = 0.02$; high-contrast, decreased by 93.4%, $P = 0.0023$; Wilcoxon signed-rank test). Our main results were consistent across animals (fig. S11) and stimulus contrast values (fig. S12,

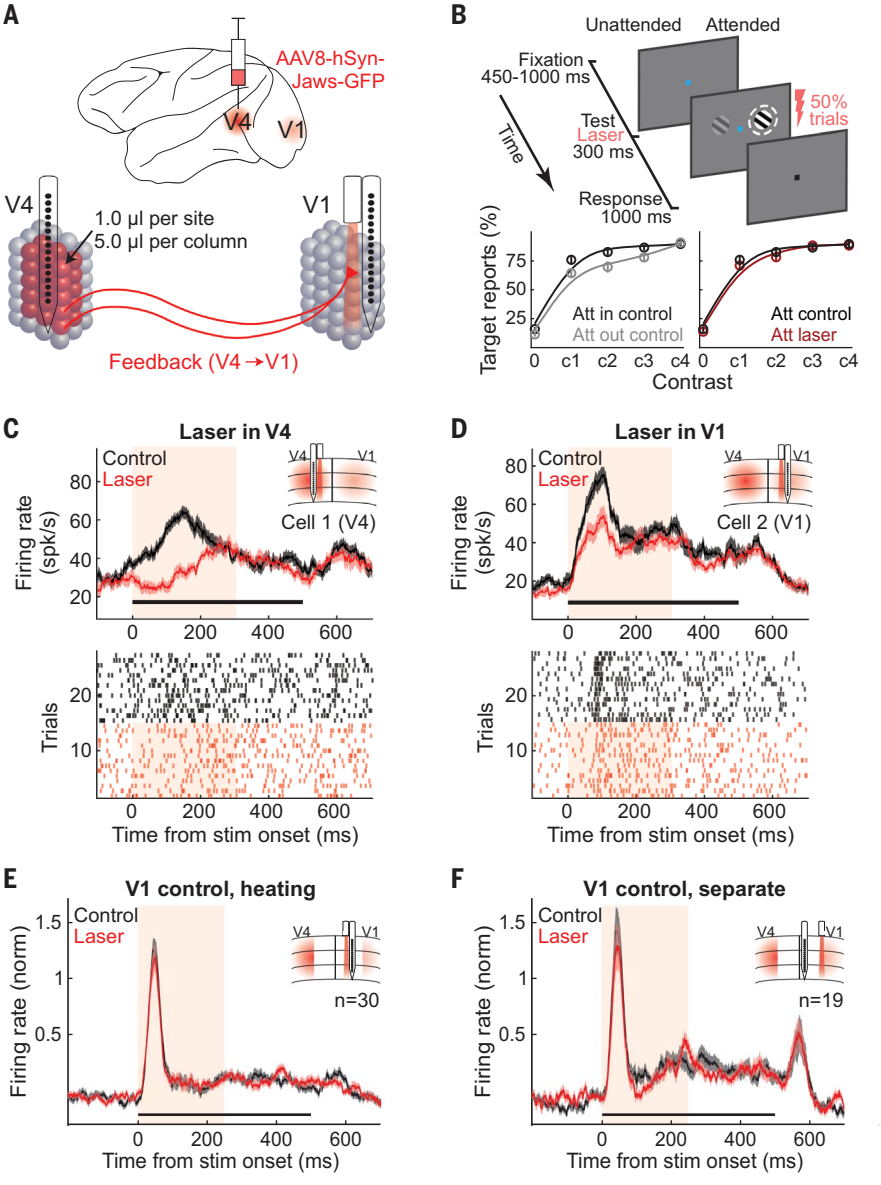

Fig. 1. Optogenetic suppression of V4 feedback axons in V1. (**A**) Schematic illustrating the AAV8-hSyn-Jaws-GFP-ER2 injection into area V4. Feedback terminals are inactivated by placing a fiber optic laser in V1. (**B**) Top: Schematic of spatial attention task. Bottom left: Behavioral performance during control (no laser) trials as a function of stimulus location, plotted with a spline curve fit (low- to high-contrast, $P = 0.11, 0.08, 0.09, 0.17, 0.56$, Wilcoxon signed-rank test). Bottom right: Behavioral performance in attended condition as a function of laser stimulation, plotted with a spline curve fit (low- to high-contrast, $P = 0.23, 0.37, 0.09, 0.59, 0.63$, Wilcoxon signed-rank test). (**C**) Peristimulus time histogram (PSTH) (top) and raster (bottom) plots for an example V4 cell when laser stimulation targets cell bodies at injection site. In all plots, the envelope represents SEM, black horizontal line represents stimulus duration, and shaded window represents laser stimulation. (**D**) PSTH (top) and raster (bottom) plots for an example V1 cell when laser stimulation targets V4 feedback terminals in V1. (**E**) Population PSTH of V1 cells ($n = 30$), recorded from a part of V1 likely not receiving transfected V4 feedback terminals. (**F**) Population PSTH of V1 cells ($n = 19$), recorded while the electrode and laser were separated (>2 mm).

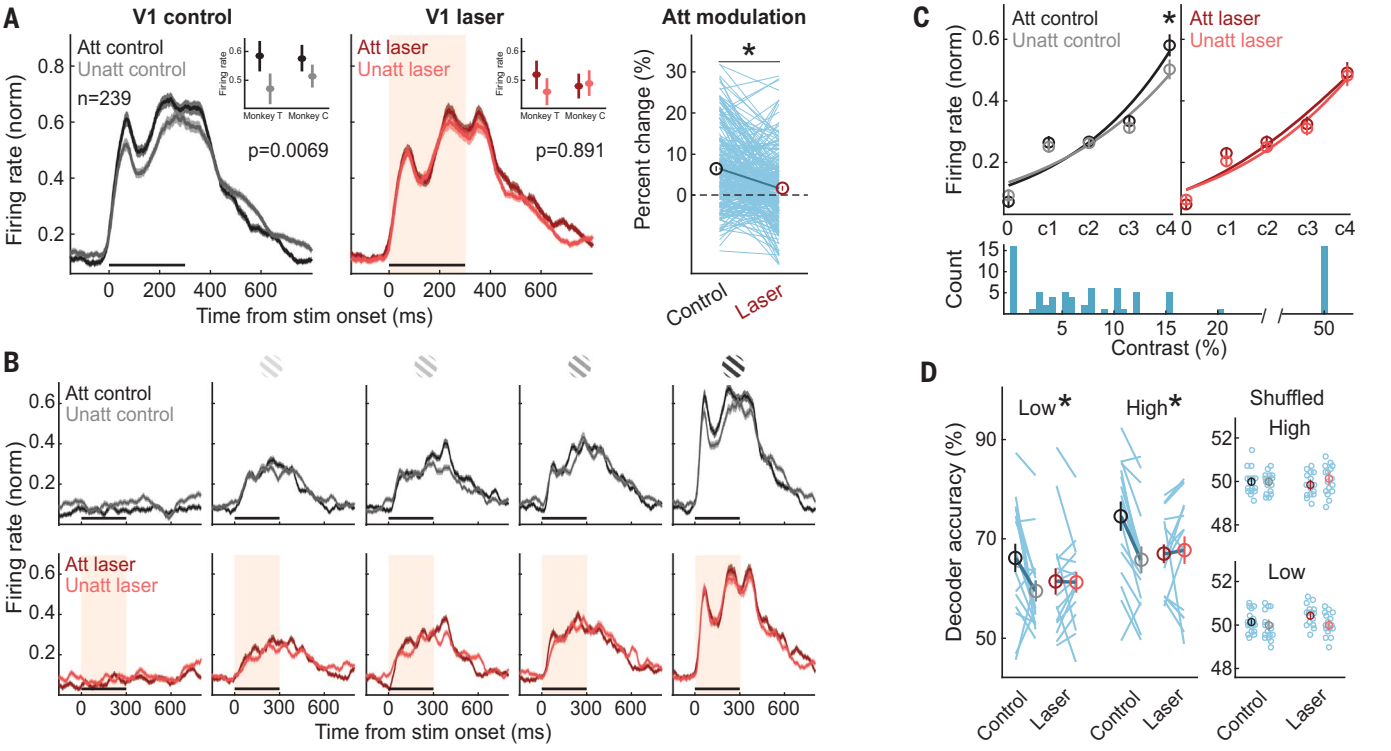

Fig. 2. V4 feedback carries attentional signals to V1. (**A**) Left: Neural responses to the high-contrast stimulus (50% contrast) flashed in cells' receptive field without laser stimulation. Population PSTH (n = 239) while animals attended the stimulus ("Att control," black) compared to when animals attended to the opposite side of the screen ("Unatt control," gray, $P = 9.59 \times 10^{-10}$, Wilcoxon signed-rank test). In all plots, the envelope represents SEM; black horizontal line represents stimulus duration. Inset shows per animal changes. Middle: Same as left panel, but during laser stimulation. Population PSTH while animals attended the stimulus ("Att laser," maroon) compared to when animals attended to the opposite side of the screen ("Unatt laser," pink, P = 0.95, Wilcoxon signed-rank test). In all plots, the shaded window represents laser stimulation. Right: Changes in attentional modulation with and without feedback as percent change of control condition effects (black) compared to laser conditions (red, $P = 3.61 \times 10^{-9}$, Wilcoxon signed-rank test). Blue lines represent values from individual cells; dark line represents the mean. (**B**) Top: Population PSTHs across all contrasts without laser stimulation. Bottom: With laser stimulation. (**C**) Top left: Population contrast response functions for control conditions, plotted with a cumulative Gaussian fit (c0, P = 0.051; c1, P = 0.20; c2, P = 0.89; c3, P = 0.25; c4, $P = 9.59 \times 10^{-10}$, Wilcoxon signed-rank test). Top right: Contrast response functions for laser conditions (c0, P = 0.055; c1 P = 0.011; c2 P = 0.081; c3 P = 0.50; c4 P = 0.95, Wilcoxon signed-rank test). Bottom: Histogram of contrasts used in all experiments. (**D**) Left: Relative difference (control versus laser) in decoder accuracy for low- and high-contrast stimuli (low, P = 0.02; high, P = 0.0023, Wilcoxon signed-rank test). Right: "Shuffled" decoder performance for low- (bottom) and high- (top) contrast stimuli. Blue lines represent values from individual sessions; dark lines represent the mean.

see supplementary materials). Analyzing the responses of all stimulus-responsive cells regardless of whether they were light-sensitive or not (n = 309 neurons) yielded highly significant effects of cortical feedback inactivation on attentional modulation of individual cell responses (fig. S13).

Laminar dependency of feedback inactivation effects

Because feedback axons from V4 preferentially terminate in the upper layers of V1 (*12*–*16*) (Fig. 3A), we asked whether the effects of feedback inactivation are layer specific. Current source-density analysis was used to assign recorded cells on the linear array to laminar locations (*26*, *27*) (Fig. 3B¸ see materials and methods). Out of 16 sessions, we identified the full laminar profile in 9 sessions, i.e., a total of 47, 44, and 32 cells in the supragranular (SG), granular (G), and infragranular (IG) layers, respectively. Attention influenced mean firing rates and decoder performance in the supragranular layers [attention modulation at c4 contrast, control versus laser, SG: P = 0.00015; Wilcoxon signed-rank test (Fig. 3C and fig. S14); SG decoder low-contrast (c1-c2): P = 0.016; SG decoder high-contrast (c3-c4): P = 0.016 (Fig. 3D and fig. S15)], although the effects in the other layers were weak and statistically nonsignificant (G attention modulation, P = 0.26; G decoder low-contrast, P = 0.55, G decoder high-contrast, P = 0.11; IG attention modulation, P = 0.36; IG decoder low-contrast, P = 1, IG decoder high-contrast, P = 0.69). The supragranular layers were significantly more influenced by feedback suppression than the granular or infragranular layers (degree of attentional modulation in control versus laser: low-contrast, P = 0.03; high-contrast, P = 0.0071, Kruskal-Wallis test, post hoc Fisher's least significant difference test). Thus, cortical feedback-inactivation effects are not generalizable to the entire cortical column.

The effects seen in SG layers were not simply due to laser position. Light scatters and becomes absorbed by the neural tissue. The red light used to activate our Jaws construct is significantly less prone to these issues than are blue- or green-light anion channelrhodopsin alternatives (*19*, *28*, *29*). We positioned the laser to directly target granular layers, but this procedure did not elicit laser-mediated firing rate changes (fig. S16). Cortical feedback thus impacts attentional modulation in V1, primarily in the supragranular layers.

Feedback-related changes in attentional modulation propagate to V4

We further tested whether optogenetically altering V4→V1 cortical feedback induces effects that propagate downstream. We recorded the

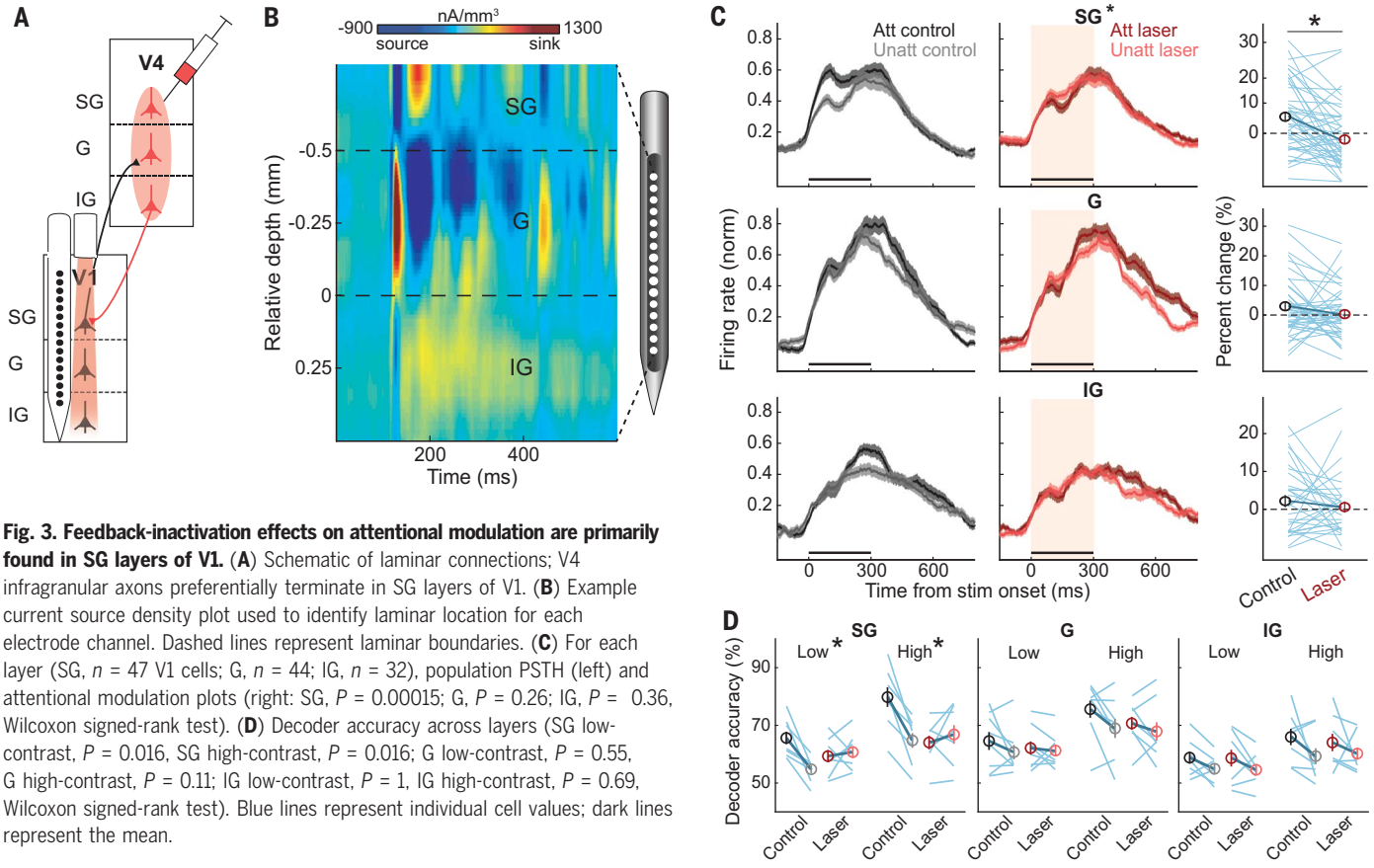

Fig. 3. Feedback-inactivation effects on attentional modulation are primarily found in SG layers of V1. (**A**) Schematic of laminar connections; V4 infragranular axons preferentially terminate in SG layers of V1. (**B**) Example current source density plot used to identify laminar location for each electrode channel. Dashed lines represent laminar boundaries. (**C**) For each layer (SG, n = 47 V1 cells; G, n = 44; IG, n = 32), population PSTH (left) and attentional modulation plots (right: SG, P = 0.00015; G, P = 0.26; IG, P = 0.36, Wilcoxon signed-rank test). (**D**) Decoder accuracy across layers (SG low-contrast, P = 0.016, SG high-contrast, P = 0.016; G low-contrast, P = 0.55, G high-contrast, P = 0.11; IG low-contrast, P = 1, IG high-contrast, P = 0.69, Wilcoxon signed-rank test). Blue lines represent individual cell values; dark lines represent the mean.

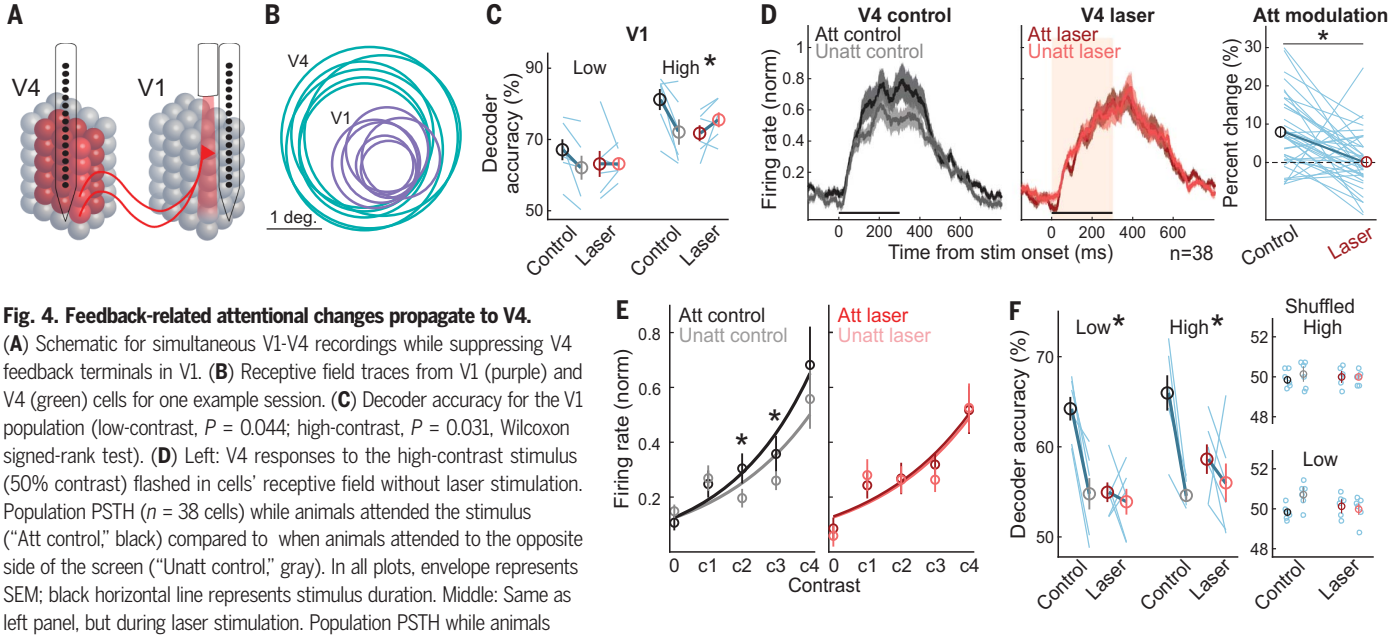

Fig. 4. Feedback-related attentional changes propagate to V4. (**A**) Schematic for simultaneous V1-V4 recordings while suppressing V4 feedback terminals in V1. (**B**) Receptive field traces from V1 (purple) and V4 (green) cells for one example session. (**C**) Decoder accuracy for the V1 population (low-contrast, P = 0.044; high-contrast, P = 0.031, Wilcoxon signed-rank test). (**D**) Left: V4 responses to the high-contrast stimulus (50% contrast) flashed in cells' receptive field without laser stimulation. Population PSTH (n = 38 cells) while animals attended the stimulus ("Att control," black) compared to when animals attended to the opposite side of the screen ("Unatt control," gray). In all plots, envelope represents SEM; black horizontal line represents stimulus duration. Middle: Same as left panel, but during laser stimulation. Population PSTH while animals attended the stimulus ("Att laser," maroon) compared to when animals attended to the opposite side of the screen ("Unatt laser," pink). In all plots, the shaded window represents laser stimulation. Right: Changes in V4 attentional modulation with and without feedback suppression as percent change of effects in control conditions (black) compared to laser conditions (red, P = 0.00033, Wilcoxon signed-rank test). Blue lines represent values from individual cells; dark line represents the mean. (**E**) Left: Contrast response functions for control condition, plotted with a cumulative Gaussian fit (c0, P = 0.015; c1, P = 0.16; c2, $P = 0.3.25 \times 10^{-5}$; c3, P = 0.00041; c4, $P = 3.9 \times 10^{-5}$, Wilcoxon signed-rank test). Right: Contrast response functions for laser condition, plotted with a Gaussian fit (c0, P = 0.057; c1, P = 0.036; c2, P = 0.86; c3, P = 0.0085; c4, P = 0.73, Wilcoxon signed-rank test). (**F**) Left: Relative V4 decoder (control versus laser) accuracy (low-contrast, P = 0.031, high-contrast, P = 0.031, Wilcoxon signed-rank test). Right: "Shuffled" decoder performance for low- (bottom) and high- (top) contrast stimuli. Blue lines represent values from individual sessions; dark lines represent the mean.

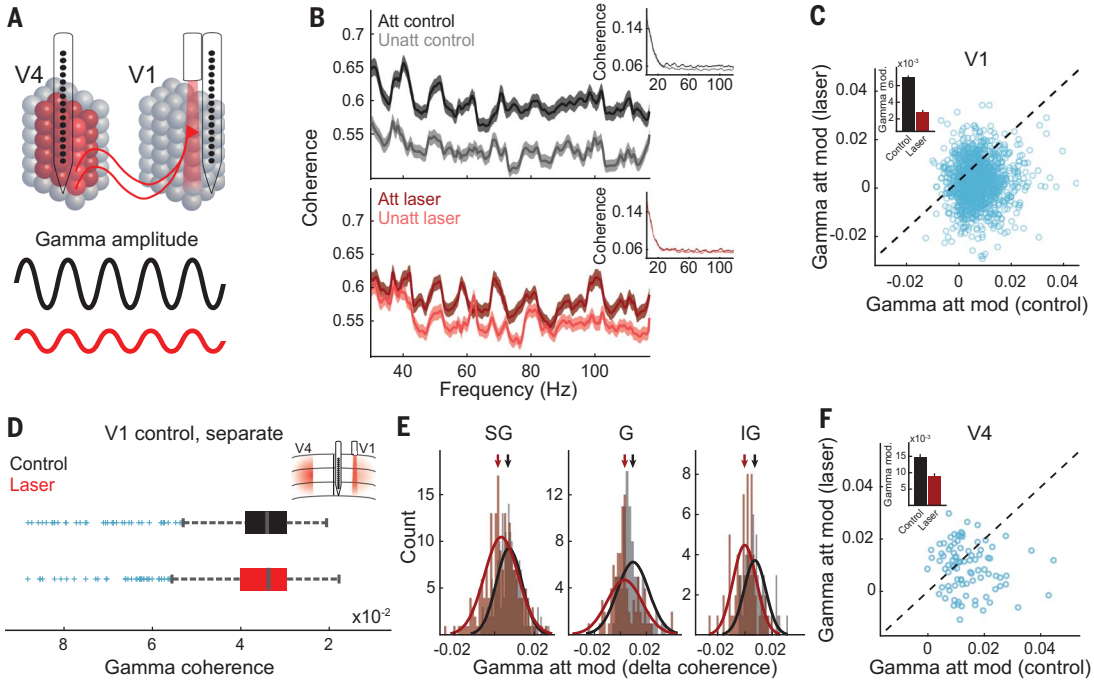

Fig. 5. Feedback-mediated attentional signals modulate gamma-coherence. (**A**) Top: Schematic of recording design. Bottom: Hypothesized changes in gamma amplitude across conditions, showing reduced gamma coherence during the laser condition. (**B**) Spike–spike gamma coherence. Insets show coherence across a wide frequency range. Top: Control conditions. Bottom: Laser conditions. For all plots, error bars reflect SEM. (**C**) Changes in V1 gamma modulation with and without feedback as attentional modulation in control versus laser conditions (n = 1,315 pairs, $P < 10^{-10}$, Wilcoxon signed-rank test). Each blue point represents one cell. Inset shows averages for control (black) and laser (red) conditions. (**D**) Box and whisker plot of gamma-coherence values during fixation (without attentional manipulation) for control (black) and laser (red) conditions while recording electrode and optic fiber were separated by >2 mm (P = 0.95, Wilcoxon signed-rank test). (**E**) Histograms show attentional modulation (relative difference between attended and unattended) of gamma coherence as a function of laser stimulation across the V1 laminae (SG: n = 194 pairs, G: n = 91, IG: n = 66), plotted with normal fits (SG: $P = 4.21 \times 10^{-7}$; G: $P = 1.20 \times 10^{-5}$; IG: $P = 2.01 \times 10^{-5}$, Wilcoxon signed-rank test). Arrows represent the mean gamma modulation (attended versus unattended) for control and laser conditions. (**F**) Changes in V4 gamma modulation with and without feedback, computed as attentional modulation in control versus laser conditions (n = 90 pairs, P = 0.00082, Wilcoxon signed-rank test). Each blue point represents one cell. Inset shows average attentional modulation (relative difference between attended and unattended) for control (black) and laser (red) conditions.

electrical activity of 38 V4 cells (six sessions in two animals, Fig. 4A) by positioning the laminar electrode to target sites localized at least 800 μm below cortical surface to maximize the likelihood of reaching the middle layers, (i.e., the recipients of feedforward inputs from early visual cortex). Simultaneously, we recorded and optically stimulated the feedback axonal terminals in V1. Cells in V1 and V4 had overlapping receptive fields and were modulated by visual stimuli (Fig. 4B). We first confirmed that in the absence of feedback suppression, attention led to a significant increase in V1 firing rates (c4 contrast control, attended versus unattended, $P = 2.74 \times 10^{-13}$), and suppressing cortical feedback rendered attended- and unattended-trial firing rates indistinguishable from one another (c4 contrast laser, attended versus unattended, P = 0.79). Comparing the effect of attention as a function of laser stimulation, we found a significant change in both firing rates and decoder accuracy (attentional modulation at c4 contrast in control versus laser: firing rate, $P = 9.6 \times 10^{-11}$; decoder low-contrast, P = 0.044, decoder high-contrast, P = 0.031, Wilcoxon signed-rank test).

We further examined whether the feedback-inactivation effects observed in V1 are transmitted to V4. In control, attention increased the mean response of V4 neurons by 9.9% (±7.49) at the highest contrast (Fig. 4D, left). Overall, the attentional modulation of V4 firing rates was significant for three out of four contrasts displayed during the task (c1, P = 0.72; c2, P = 0.00027; c3, P = 0.049; c4, P = 0.00033), confirming the expectation that the effects of attention are more prominent in V4 compared to V1 (where firing rates were only significantly different for the high-contrast stimulus). Suppressing cortical feedback to V1 reduced the attentional gain response in V4 [c4 contrast: Fig. 4, D (middle) and E]. The relative differences between these conditions (control versus laser) indicate that the attention-induced increase in neural responses critically relies on feedback signals [firing rate: P = 0.00033 (Fig. 4D, right); decoder low-contrast: P = 0.031, high-contrast: P = 0.031 (Fig. 4F and fig. S17)]. This result is surprising, as downstream prefrontal areas also send feedback inputs to the superficial layers of V4 that are believed to carry attentional signals. However, our electrode penetrations have likely oversampled the granular layers to possibly explain the light-induced reduction in attentional modulation in V4.

Feedback-mediated attentional signals modulate gamma coherence

Because attention has been commonly associated with increased gamma activity in visual cortex (*30*–*33*), we investigated whether the selective suppression of V4→V1 feedback terminals influences gamma spike–spike coherence in V1 (*18*, *34*, *35*) (Fig. 5A). In the absence of light, attention was associated with increased gamma coherence (attended versus unattended, 6.3%, $P < 10^{-10}$), both in the low- (30 to 80 Hz, $P < 10^{-10}$) and high-gamma frequency bands (80 to 120 Hz, $P = 2.16 \times 10^{-80}$). However, when cortical feedback was optogenetically suppressed (Fig. 5B, bottom), the attention-mediated changes were much reduced, leading to a 2.5-fold decrease in gamma coherence [control versus laser, $P = 1.01 \times 10^{-35}$, Wilcoxon signed-rank test (Fig. 5C); this effect was consistent across animals (fig. S18), and the attentional modulation of spike coherence in nearby frequency bands was not significantly influenced by feedback inactivation (beta, P = 0.074; alpha, P = 0.97, Wilcoxon signed-rank test)]. This effect was indeed driven by feedback signals, as separating the recording probe and optic fiber by several millimeters during a fixation task did not elicit significant changes in gamma coherence between the attended and unattended conditions (P = 0.95) (Wilcoxon signed-rank test, Fig. 5D).

We next investigated whether the attention-induced changes in gamma coherence are layer specific. The relative change in gamma

coherence between control and laser conditions (attended versus unattended) was significantly modulated in all layers (SG: $P = 4.21 \times 10^{-7}$; G: $P = 1.20 \times 10^{-5}$; IG: $P = 2.01 \times 10^{-5}$) (Fig. 5E) despite the fact that the effects on neuronal responses and network performance are layer-dependent. Finally, we computed spike–spike coherence between pairs of V4 cells, as V4 responses were strongly influenced by cortical feedback suppression (Fig. 3). Suppressing cortical feedback to V1 significantly reduced attentional modulation (attended versus unattended) of gamma coherence across pairs of V4 cells ($P = 0.00082$, Fig. 5F).

Discussion

For the past several decades, neuroscientists have widely assumed that cortical feedback mediates attentional modulation in brain circuits. Because this hypothesis is intuitive, it has long dominated research in the field despite lack of direct support. Previous studies have either demonstrated attention-related interactions between cortical areas without establishing causality (*5*, *36*–*39*) or used causal manipulations to perturb cortical feedback without measuring attentional signals (*1*, *3*, *8*, *9*, *40*). Furthermore, previous studies have largely ignored laminar-specific changes, although it is well accepted that feedback connections are layer-specific, and hence their effects on neuronal responses may vary across the targeted cortical column.

Our findings provide causal evidence of attentional modulation in individual neurons and cell populations induced by cortical feedback projections. Optogenetically suppressing V4 feedback axons to V1, without inherently altering local and feedforward intracortical inputs, significantly diminished the attention-induced benefits on response gain and accuracy of network computations, abolished attentional modulation of postsynaptic V4 neuron responses, and greatly reduced gamma coherence when attention was deployed. Our results further indicate that feedback signals modulate visual cortical responses only when stimuli are attended.

It has been hypothesized that the pulvinar may constitute one source of attentional modulation of neuronal responses in early cortex (*41*, *42*). Specifically, the pulvinar may synchronize neuronal responses across cortical areas by attention allocation and hence regulate information transmission. However, although our results do not challenge this view, they raise the possibility that cortical feedback and the pulvinar could work together to fulfill optimal attentional requirements during visual perception. Further research is needed to tease apart attentional influences due to pulvinar and cortical feedback sources.

Our findings may have general implications applicable to the entire cortex, because they suggest that cortical feedback connections carry attentional signals via laminar-specific mechanisms. Thus, our results could set the stage for further investigations probing large-scale feedback circuits across species to study the effects of attention at multiple stages of thalamic and cortical processing. Because feedback has been hypothesized to control other top-down processes, such as expectation and behavioral context, our results could have widespread implications for a broad range of phenomenology across many modalities.

REFERENCES AND NOTES

1. J. M. Hupé *et al*., *Nature* **394**, 784–787 (1998).
2. T. Moore, K. M. Armstrong, *Nature* **421**, 370–373 (2003).
3. J. J. Nassi, S. G. Lomber, R. T. Born, *J. Neurosci.* **33**, 8504–8517 (2013).
4. L. B. Ekstrom, P. R. Roelfsema, J. T. Arsenault, G. Bonmassar, W. Vanduffel, *Science* **321**, 414–417 (2008).
5. B. Dagnino, M.-A. Gariel-Mathis, P. R. Roelfsema, *J. Neurophysiol.* **113**, 730–739 (2015).
6. A. F. Rossi, N. P. Bichot, R. Desimone, L. G. Ungerleider, *J. Neurosci.* **27**, 11306–11314 (2007).
7. B. Noudoost, K. L. Clark, T. Moore, *J. Neurosci.* **34**, 3687–3698 (2014).
8. J.-M. Hupé, A. C. James, P. Girard, J. Bullier, *J. Neurophysiol.* **85**, 146–163 (2001).
9. J. H. Sandell, P. H. Schiller, *J. Neurophysiol.* **48**, 38–48 (1982).
10. T. van Kerkoerle *et al*., *Proc. Natl. Acad. Sci. U.S.A.* **111**, 14332–14341 (2014).
11. P. C. Klink, B. Dagnino, M. A. Gariel-Mathis, P. R. Roelfsema, *Neuron* **95**, 209–220.e3 (2017).
12. L. G. Ungerleider, T. W. Galkin, R. Desimone, R. Gattass, *Cereb. Cortex* **18**, 477–499 (2008).
13. D. J. Felleman, D. C. Van Essen, *Cereb. Cortex* **1**, 1–47 (1991).
14. K. S. Rockland, K. S. Saleem, K. Tanaka, *Vis. Neurosci.* **11**, 579–600 (1994).
15. J. Bullier, H. Kennedy, W. Salinger, *J. Comp. Neurol.* **228**, 329–341 (1984).
16. G. H. Henry, P. A. Salin, J. Bullier, *Eur. J. Neurosci.* **3**, 186–200 (1991).
17. E. A. Buffalo, P. Fries, R. Landman, H. Liang, R. Desimone, *Proc. Natl. Acad. Sci. U.S.A.* **107**, 361–365 (2010).
18. J. F. Mitchell, K. A. Sundberg, J. H. Reynolds, *Neuron* **63**, 879–888 (2009).
19. A. S. Chuong *et al*., *Nat. Neurosci.* **17**, 1123–1129 (2014).
20. L. Acker, E. N. Pino, E. S. Boyden, R. Desimone, *Proc. Natl. Acad. Sci. U.S.A.* **113**, E7297–E7306 (2016).
21. X. Han *et al*., *Neuron* **62**, 191–198 (2009).
22. C. D. Gilbert, W. Li, *Nat. Rev. Neurosci.* **14**, 350–363 (2013).
23. B. C. Motter, *J. Neurophysiol.* **70**, 909–919 (1993).
24. J. H. Reynolds, L. Chelazzi, *Annu. Rev. Neurosci.* **27**, 611–647 (2004).
25. Y. Chen *et al*., *Nat. Neurosci.* **11**, 974–982 (2008).
26. C. E. Schroeder, A. D. Mehta, S. J. Givre, *Cereb. Cortex* **8**, 575–592 (1998).
27. K. H. Pettersen, A. Devor, I. Ulbert, A. M. Dale, G. T. Einevoll, *J. Neurosci. Methods* **154**, 116–133 (2006).
28. O. Yizhar, L. E. Fenno, T. J. Davidson, M. Mogri, K. Deisseroth, *Neuron* **71**, 9–34 (2011).
29. T. Vo-Dinh, Ed., *Biomedical Photonics Handbook* (CRC Press, ed. 2, 2003).
30. P. Fries, J. H. Reynolds, A. E. Rorie, R. Desimone, *Science* **291**, 1560–1563 (2001).
31. P. Fries, T. Womelsdorf, R. Oostenveld, R. Desimone, *J. Neurosci.* **28**, 4823–4835 (2008).
32. T. Womelsdorf, P. Fries, P. P. Mitra, R. Desimone, *Nature* **439**, 733–736 (2006).
33. N. P. Bichot, A. F. Rossi, R. Desimone, *Science* **308**, 529–534 (2005).
34. J. L. Herrero, M. A. Gieselmann, M. Sanayei, A. Thiele, *Neuron* **78**, 729–739 (2013).
35. S. Ray, J. H. R. Maunsell, *Neuron* **67**, 885–896 (2010).
36. D. Ferro, J. van Kempen, M. Boyd, S. Panzeri, A. Thiele, *Proc. Natl. Acad. Sci. U.S.A.* **118**, e2022097118 (2021).
37. J. D. Semedo *et al*., *Nat. Commun.* **13**, 1099 (2022).
38. J. Moran, R. Desimone, *Science* **229**, 782–784 (1985).
39. A. Speed, J. Del Rosario, N. Mikail, B. Haider, *Nat. Commun.* **11**, 505 (2020).
40. L. Nurminen, S. Merlin, M. Bijanzadeh, F. Federer, A. Angelucci, *Nat. Commun.* **9**, 2281 (2018).
41. Y. B. Saalmann, M. A. Pinsk, L. Wang, X. Li, S. Kastner, *Science* **337**, 753–756 (2012).
42. I. C. Fiebelkorn, S. Kastner, *Annu. Rev. Psychol.* **71**, 221–249 (2020).

ACKNOWLEDGMENTS

We thank A. Andrei for technical assistance, A. Asadollahi for help with control experiments, R. Janz for help with virus handling and expression, S. Pojoga for help with the design of the behavioral task, and A. Parajuli for discussions on control analyses. **Funding:** National Eye Institute grant 1F31EY030735-01 (S.R.D.), NIH BRAIN Initiative grant 1R34NS116829 (V.D.). **Author contributions:** Conceptualization: S.R.D., V.D. Methodology: S.R.D., V.D. Investigation: S.R.D., V.D. Visualization: S.R.D., V.D. Funding acquisition: S.R.D., V.D. Project administration: S.R.D., V.D. Supervision: V.D. Writing – original draft: S.R.D., V.D. Writing – review and editing: S.R.D., V.D. **Competing interests:** The authors declare no competing financial interests. Correspondence and requests for materials should be addressed to V.D. (valentin.dragoi@uth.tmc.edu). **Data and materials availability:** All data supporting the findings from this study are openly available at https://zenodo.org/record/7297037#.Y2g5uHbMKUk.

SUPPLEMENTARY MATERIALS

science.org/doi/10.1126/science.ade1855
Materials and Methods
Supplementary Text
Figs. S1 to S18
References (*43*–*46*)
MDAR Reproducibility Checklist

View/request a protocol for this paper from *Bio-protocol*.

Submitted 29 July 2022; accepted 23 December 2022
10.1126/science.ade1855